Analysis of Rayleigh-Lamb Modes in Soft-solids with Application to Surface Wave Elastography

Nicolás Benech, Gustavo Grinspan, Sofía Aguiar, Javier Brum, Carlos Negreira, Mickäel Tanter, Jean-Luc Gennisson

Available online at www.sciencedirect.com

ScienceDirect

Physics Procedia 70 (2015) 175 – 178

Physics Procedia

2015 International Congress on Ultrasonics, 2015 ICU Metz

Analysis of Rayleigh-Lamb modes in soft-solids with application to surface wave elastography

Nicolás Benech[a]*, Gustavo Grinspan[b], Sofía Aguiar[c], Javier Brum[a], Carlos Negreira[a] Mickäel tanter[d] and Jean-Luc Gennisson[d]

[a]*Laboratorio de Acústica Ultrasonora, Instituto de Física, Facultad de Ciencias, Igua 4225, 11400, Montevideo, Uruguay*
[b]*Sección Biofísica, Instituto de Biología, Facultad de Ciencias, Igua 4225, 11400, Montevideo, Uruguay*
[c]*Instituto de ensayo de materiales, Facultad de Ingeniería, Julio Herrera y Reisig 565, 11300, Montevideo, Uruguay*
[d]*Institut Langevin, ESPCI ParisTech, PSL Research University, CNRS UMR7587, INSERM U979, 1 Rue Jussieu, Paris, France*

Abstract

The goal of Surface Wave Elastography (SE) techniques is to estimate the shear elasticity of the sample by measuring the surface wave speed. In SE the thickness of the sample is often assumed to be infinite, in this way, the surface wave speed is directly linked to the sample's shear elasticity. However for many applications this assumption is not true. In this work, we study experimentally the Rayleigh-Lamb modes in soft solids of finite thickness to explore the optimal conditions for SWE. Experiments were carried out in three tissue mimicking phantoms of different thicknesses (10 mm, 20 mm and 60 mm) and same shear elasticity. The surface waves were generated at the surface of the phantom using piston attached to a mechanical vibrator. The central frequency of the excitation was varied between 60 Hz to 160 Hz. One component of the displacement field generated by the piston was measured at the surface and in the bulk of the sample trough a standard speckle tracking technique using a 256 element, 7.5 MHz central frequency linear array and an ultrasound ultrafast electronics. Finally, by measuring the phase velocity at each excitation frequency, velocity dispersion curves were obtained for each phantom. The results show that instead of a Rayleigh wave, zero order symmetric (S_0) and antisymmetric (A_0) Lamb modes are excited with this type of source. Moreover, in this study we show that due to the near field effects of the source, which are appreciable only in soft solids at low frequencies, both Lamb modes are separable in time and space. We show that while the Ao mode dominates close the source, the S_0 mode dominates far away.

Peer-review under responsibility of the Scientific Committee of ICU 2015

* Corresponding author. Tel.: +59825258624; fax: +59825250580.
E-mail address: nbenech@fisica.edu.uy

Peer-review under responsibility of the Scientific Committee of ICU 2015
doi:10.1016/j.phpro.2015.08.104

1. Introduction

Assessing the mechanical parameters of soft-solids from surface wave velocity measurements is an active field of research in elastography. Despite elasticity imaging systems are now commercially available, they are still unaffordable for many applications where a global elasticity measurement is required instead of an elasticity image. A non-exhaustive list includes quality controls in the food industry (Brum 2009, Benech 20102a) and diagnosis of musculoskeletal disorders where usually subjective palpation techniques are applied to assess muscle stiffness (Benech 2012b, Salman 2013). Therefore, low-cost surface wave methods emerge as an alternative to more sophisticated imaging systems. Generally, the surface wave is generated by a mechanical low-frequency (20 – 200 Hz) source acting on the surface of the sample. The surface wave is then detected by two or more sensors (e.g. accelerometers, passive piezoelectric sensors, etc.) located at different positions on the surface of the sample (Brum 2008). In addition, non-contact measuring systems like laser Doppler vibrometry or optical methods were reported (Salman 2013, Benech 2005). Whatever the measuring system, it is assumed that the Surface Wave Velocity (SWV) is related in a simple way to the shear wave speed β which is directly linked to the shear modulus μ through $\mu = \rho \beta^2$ (ρ being the density of the material). Under this assumption, a high SWV value indicates a high value of μ. However, since samples are finite-sized, usually guided wave modes propagates along the surface. Consequently, the measured SWV will depend on the dimensionless parameter $\varepsilon = fh/\beta$, where f is the frequency of the wave and h samples' height. This dependence prevents to compare inter-sample measurements and only relative elasticity changes of the same sample can be reported. Therefore, a technique capable of measuring the absolute elasticity value would benefit inter-sample comparisons and the whole technique. The aim of this work is to give a step in that direction.

2. Experimental setup

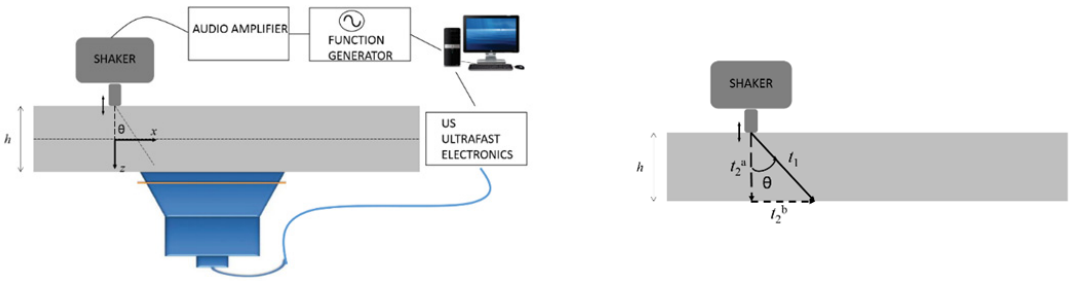

Fig 1. a) Schematic of the experimental setup where the low-frequency source and the US probe are shown. b) Diagram showing two different arrival paths to a particular position within the lower surface. The path labelled with t_1 is the direct shear wave while the path labelled with t_2^a and t_2^b indicates a wave that arrives at the lower surface and then propagates along the surface.

Figure 1a displays a schematic of the experimental setup. Three tissue mimicking phantoms of heights h = 10, 20 and 60 mm were made from the same mixture of agar-gelatin (2% agar, 3% gelatin), i.e. same shear elasticity. The length (185 mm) and width (120 mm) were the same for the three samples. The surface wave was generated by a 7.5-mm-diameter piston attached to a mechanical vibrator working from 60 to 120 Hz with a 20 Hz step acting normally to the surface of the sample. For each frequency, the vibrator was excited with a two-cycle sinusoid at the corresponding central frequency. The transient displacement field generated by the piston was measured at the surface and in the bulk of the sample trough a standard speckle tracking technique using a 256 element, 0.2 mm pitch, 7.5 MHz central frequency linear array and a home-made ultrasound ultrafast research prototype working at a frame rate of 2 kHz. The phantoms were hold up from the sides such as they have two free surfaces. The low-frequency source was placed on the upper surface while the ultrasonic array was placed in the lower one so that the first element of the array is aligned with the piston as indicated in Fig. 1a. A layer of coupling gel was put between the phantom and the probe in order to assess the lower surface displacements. This configuration allows measuring

the z component of the elastic field ($u_z(x,z,t)$) in the x,z plane as function of time. The shear wave speed value measured through 1D transient elastography is $\beta = 4.68 \pm 0.08\ m/s$.

3. Experimental results and discussion

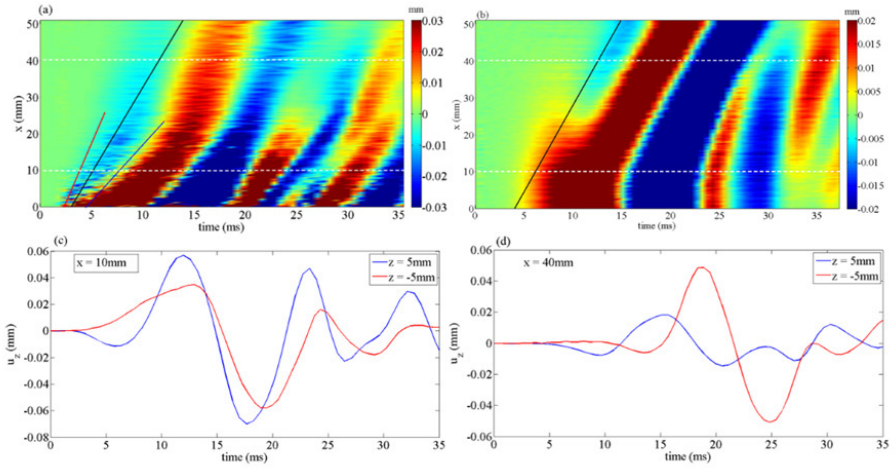

Fig 2. Displacement field as function of x and t measured at (a) the upper surface (z = -5 mm) and (b) the lower surface (z = 5 mm). Comparison of the displacement as function of t for (c) x = 10 mm and (d) x = 40 mm.

The propagation modes are due to the interactions between the reflected (and mode conversion of) P and S-waves along the sample. Since the speed of the P wave is 1500 m/s and given a frame per second of 2 kHz this wave practically propagates "instantaneously" throughout the phantom. Therefore, due to the low speed of the S-wave (~5 m/s), it will always interact with the P-wave. Figures 2a and 2b show the 100 Hz surface displacement field $u_z(x,t)$ for the 10 mm height phantom at the upper (z = -5 mm) and at the lower (z = 5 mm) surface respectively. The colorbar in these figures was set in order to the smaller amplitude waves to be visible. A full black line corresponding to a propagation speed of 4.68 m/s was included in these figures as reference. We can see in fig 2a that a negative displacement cycle is the first wave to arrive followed by a strong positive one. As is clear in the figure, the former propagates faster than the shear wave speed (full red line) while the second propagates slower (full blue line) between x = 0 and 25 mm. Fig 2c and d show a comparison of the displacement of the upper and lower surface for x = 10 and 40 mm respectively. In fig 2c we observe that the displacements are out of phase until t = 6 ms. After that, they are in phase. For x = 40 mm (fig 2d), the displacements are out of phase for all values of time. Our interpretation of this observation is that the source excites both symmetric and antisymmetric modes. It is worth noticing here that, since the source first acts in the positive z direction, the P and S displacement along the surface are negative while the Rayleigh wave is positive. Therefore, the first negative cycle of the upper surface of fig 2c is a consequence of the interaction of (direct and reflected) P and S waves. This interaction gives rise to a symmetric mode, which propagates faster than the shear wave speed. For t > 6ms, the interaction of Rayleigh, S and P waves dominate the field. Thus, until approximately x = 25 mm, the displacement on both surfaces are in phase, exciting an antisymmetric mode. However, for x > 25 mm the displacement of the lower surface changes its sign and is negative (t ~ 11ms) while in the upper surface it is still positive. These experimental observation can be explained taking into account the near-field effects of the source. For the excitation frequency used, the shear wave wavelength is approximately 47 mm. Therefore, most of our experimental data lie within the near-field of the source (Sandrin 2004). It has been shown before that the phase speed of the near-field term C_{NF} depends of the polar angle θ (defined in fig. 1) as (Benech 2013):

$$C_{NF} = \frac{3}{4}\beta(1 + \cos^2(\theta)) \quad (1)$$

Thus, apart for the P-wave, the first wave arriving to the lower surface is the near-field S-wave below the source (θ = 0). This wave, propagating with positive displacement within the bulk, produces a negative displacement S-wave on the lower surface (S_L). Thus, at a given position x of the lower surface, we may compute two arrival times depicted in fig 1b: the time t_1 of the direct near-field S-wave with positive displacement and the time t_2 of surface S_L wave which is the sum of times t_2^a and t_2^b as shown in fig 1b:

$$t_1 = (4\sqrt{(h^2 + x^2)^3})/3\beta(2h^2 + x^2)\,; \quad t_2 = 2h/3\beta + x/\beta \tag{2}$$

These two arrival times are equal at a distance that we call x_c. After some algebra, we found that $x_c \approx 23\ mm$ for h = 10 mm and $x_c \approx 46\ mm$ for h = 20 mm. Thus, for $x > x_c, t_2 < t_1$ and the surface S_L wave arrives earlier than the direct S wave. Fig. 3a displays the SWV as function of $\epsilon = fh/\beta$ measured for $x < x_c$ on the upper surface for the three phantoms and all the excitation frequencies. The full line corresponds the theoretical A_0 mode. Fig. 3b displays the SWV as function of ϵ for $x > x_c$. Since $x_c > 50\ mm$ for the 60 mm height phantom, the results for this phantom are not included in the figure. The full line is the theoretical S_0 mode. This last result shows the existence of a critical distance separating the symmetric from the antisymmetric mode related to near-field effects.

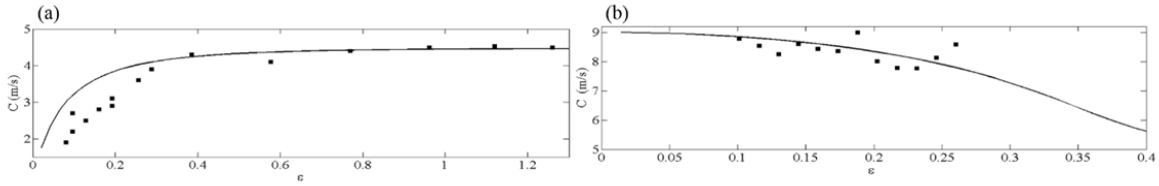

Fig 3. SWV as function of ϵ for (a) $x < x_c$ and (b) $x > x_c$. The full lines represent the theoretical A0 and S0 modes respectively.

4. Conclusions

In this work we have shown that a low-frequency point-like source acting normally on the free surface of a soft solid produces symmetric and antisymmetric Rayleigh-Lamb modes. Although the antisymmetric mode dominates the field, the symmetric mode can be measured and separated in space and time of the antisymmetric one. We show the existence of a critical distance separating the two modes. This distance is related to the near-field effects of the elastic field and is not relevant for $\epsilon \geq 1$ (i.e when $h \geq \lambda_s$). This result may have consequences in SE applications, in particular when absolute elasticity values are required instead of relative elasticity changes.

Acknowledgements

This work was supported by CSIC and PEDECIBA-Física, Uruguay.

References

Benech *et al* 2005, Elastographic parameters by surface wave analysis, Proc. IEEE Ultrasonic Symp. 1364-1367.
Benech *et al* 2012a, Elastografía ultrasónica para la evaluación de terneza en carne vacuna, PROCISUR Publicaciones, 29-44, Montevideo.
Benech *et al* 2012b, In vivo assessment of muscle mechanical properties using a low cost surface wave method, Proc. IEEE Ultrasonic Symp. 2571-2573.
Benech *et al* 2013, Near-field effects in Green's function retrieval from cross-correlation of elastic fields: Experimental study with application to elastography, J. Acoust. Soc. Am., 133, 2755-2766
Brum *et al* 2008, Shear elasticity estimation from surface wave: The time-reversal approach, J. Acoust. Soc. Am.,124, 3377-3380.
Brum *et al* 2009, Aplicación de elastografía por retorno temporal a la evaluación de textura en quesos, INNOTEC 4, 37-40.
Salman *et al* 2013, Surface wave measurement using a single continuously scanning laser doppler vibrometer: Application to elastography, J. Acoust. Soc. Am.,133, 1245-1254.
Sandrin *et al* 2004, The role of the coupling term in transient elastography, J. Acosut. Soc. Am., 115, 73-83.